

Depth from Scattering

Fabio Cozman Eric Krotkov
Robotics Institute, Carnegie Mellon University, Pittsburgh
{ fgcozman, epk } @cs.cmu.edu
<http://www.cs.cmu.edu/~{ fgcozman, epk }>

Abstract

Light power is affected when it crosses the atmosphere; there is a simple, albeit non-linear, relationship between the radiance of an image at any given wavelength and the distance between object and viewer. This phenomenon is called atmospheric scattering and has been extensively studied by physicists and meteorologists. We present the first analysis of this phenomenon from an image understanding perspective: we investigate a group of techniques for extraction of depth cues solely from the analysis of atmospheric scattering effects in images. Depth from scattering techniques are discussed for indoor and outdoor environments, and experimental tests with real images are presented. We have found that depth cues in outdoor scenes can be recovered with surprising accuracy and can be used as an additional information source for autonomous vehicles.

1 Introduction

Observers of outdoor scenery witness a variety of atmospheric effects caused by light scattering: the sky is blue, distant mountains appear bluer than nearby mountains, a flashlight beam is reflected back by a foggy environment. Such phenomena have been actively studied by physicists, meteorologists and navigators [7, 8]. In this paper, we present the first analysis of atmospheric scattering from an image understanding perspective. We investigate techniques that extract depth cues from atmospheric scattering effects in images. We use the phrase *depth from scattering* to refer to such techniques.

Investigators have studied atmospheric scattering with distinct goals. Physicists and navigators seek to predict how a particular atmosphere affects visual perception; computer graphics researchers simulate scattering rather than measure its effect in practice [4, 6]. Artists have used simulated atmospheric effects in paintings at least since the Renaissance [1]. Our purpose is new: we use atmospheric scattering as a beneficial source of information about geometric rela-

tionships among objects and a viewer.

Light power and intensity are modified principally by scattering when light crosses the atmosphere. The presence of small particles suspended in the atmosphere causes the light to scatter in a variety of directions. Given a number of assumptions discussed in the paper, we derive a relationship between the radiance of an image at any given wavelength and the distance between object and viewer. Section 2 is devoted to the derivation of this model.

The inter-dependence of scattering and distance opens the possibility of recovering depth cues from images. We investigate the application of depth from scattering techniques in indoor and outdoor environments, discussing the extent to which the assumptions indicated in the modeling stage are fulfilled (section 3). We have found that depth cues in outdoor scenes can be recovered with surprising accuracy. Our experiments and results are described in sections 4 and 5.

2 Light Scattering

Light scattering occurs when light interacts with particles suspended in the atmosphere. Effects of scattering are felt daily as we perceive the sky to be blue or reddish, depending on atmospheric conditions and solar illumination. The first successful model of scattering was developed by Lord Rayleigh in 1871, after a long period where researchers postulated that the sky was blue due to the presence of water in the atmosphere [7].

If particles in the atmosphere are spherical or small, light is scattered symmetrically with respect to incident rays of light [4]. We represent the portion of light that is scattered by a function $B(\lambda, \theta)$, the angular scattering function. The variable θ is the angle between the incident ray of light and the emanating ray of light; λ is the wavelength.

Assumption 1 *The scattering function is symmetric with respect to the incident ray of light (depends only on λ and θ).*

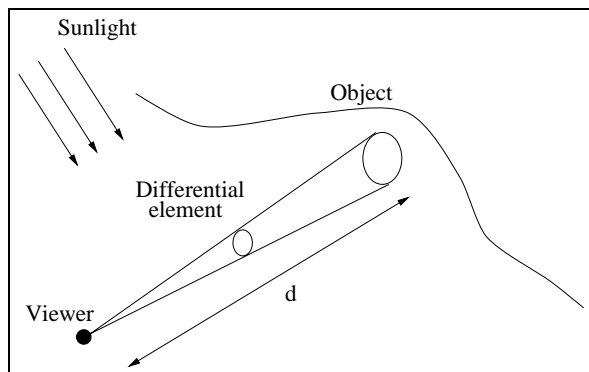


Figure 1: Light travels from an object to a viewer through the atmosphere under uniform illumination (sunlight)

Atmospheric scattering manifests itself through two phenomena, which we discuss separately. The first phenomenon is attenuation of power; the second phenomenon is sky intensity.

2.1 Attenuation of power

Take a beam of light projected through a scattering medium, as illustrated in Figure 1. The distance between object and viewer is d . As rays of light are deflected by particles, the power of light conveyed by the beam decreases. For a differential portion of the trajectory, power decreases as $dP = -\beta P dd$ [7], where $P_o(\lambda)$ is the power of the source and $\beta(\lambda)$ is called the *extinction* coefficient¹. By integration through the whole path, the received power intensity is given by:

$$P(\lambda) = P_o(\lambda) \exp(-\beta(\lambda)d). \quad (1)$$

We are interested in the intensity of an image taken by the viewer. Two factors affect the relationship between power and intensity. Power decreases with distance by the inverse square law so power decreases with d^2 ; on the other hand, intensity at a receiver increases with square of distance d^2 , because the solid angle subtended by the receiver corresponds to a larger area on the object [3]. Appendix A shows how the two effects cancel each other, so that the dependency of distance remains restricted to the exponential term.

For an object with intensity $I_o(\lambda)$ in the absence of scattering and distance d from the viewer, the intensity measured by the viewer $I(\lambda)$ is:

$$I(\lambda) = I_o(\lambda) \exp(-\beta(\lambda)d). \quad (2)$$

¹Atmospheric absorption is incorporated into this model by a slight increase in the value of β [8].

2.2 Sky intensity

Even though light power is attenuated by direct scattering, there is another effect, also due to scattering, which increases the power in a light beam. We now model this phenomenon using some additional assumptions.

Consider an imaginary line, traced from the viewer to some point infinitely far away in a scattering medium. Suppose the line is illuminated by a uniform source from the top (for example, the sky). At each point of the line, scattering events take place and divert light from its original path.

As light is directed to the viewer from all points in the line, the viewer perceives a new source of light, due exclusively to scattering.

From the previous sections, we know that the light coming from any point at distance x is affected by the angular scattering function and is attenuated exponentially. To obtain the amount of light received in this manner, we integrate the effect of scattering events from the viewer to an arbitrary distance d :

$$I(\lambda) = \int_0^d I_o(\lambda) B(\lambda, \theta) \exp(-\beta(\lambda)x) dx,$$

which leads to:

$$I(\lambda) = \frac{I_o(\lambda) B(\lambda, \theta)}{\beta(\lambda)} (1 - \exp(-\beta(\lambda)d)).$$

The integration assumes:

Assumption 2 *Illumination from the sky is uniform and rays of light from the sky are all parallel.*

Assumption 3 *Each ray of light is scattered once.*

The first assumption is reasonable for the sky, and can possibly be approximated in large indoor environments. The second assumption is an approximation based on empirical observations [8].

In order to reduce the complexity of the scattering model above, we make the following assumption:

Assumption 4 *The variation of θ across an object located relatively far away is small enough so that its effect in $\frac{I_o(\lambda) B(\lambda, \theta)}{\beta(\lambda)}$ is negligible.*

Under this assumption, call *sky intensity* $S(\lambda)$ the quantity $\frac{I_o(\lambda) B(\lambda, \theta)}{\beta(\lambda)}$. If a viewer were to look at a point infinitely far away ($d \rightarrow \infty$), the perceived intensity would be $S(\lambda)$, solely caused by atmospheric scattering.

2.3 Combining scattering effects

The two effects above, attenuation and sky intensity, are additive due to the linear character of light propagation [8]. Suppose an object located at distance d has intensity $I_o(\lambda)$ when imaged in a vacuum. In the presence of atmosphere the intensity is:

$$I(\lambda) = \exp(-\beta(\lambda)d)I_o(\lambda) + (1 - \exp(-\beta(\lambda)d))S(\lambda).$$

So far we have kept the dependencies on wavelength λ explicit. In a non-polluted atmosphere, without rain or snow, scattering is mainly caused by small particles and is sensitive to the wavelength². Variations across wavelength are small, and can only be perceived distinctly for large distances. For the distances involved in our experiments (between 1000 to 3000 meters), there is no appreciable “blueing” effect. For larger particles, wavelength selectivity decreases remarkably. For dense concentrations of clean water droplets such that visibility falls below 1000 meters (a situation defined as fog [8]), the dependence on wavelength becomes negligible. Due to such considerations, we drop the dependency on λ in the remainder of this paper, since it has no effect relevant to our experiments. We refer to the *measured* intensity of an object as \tilde{C} , and the intensity of the object without scattering as C . We arrive at our basic equation:

$$\tilde{C} = C \exp(-\beta d) + S(1 - \exp(-\beta d)). \quad (3)$$

3 Depth from Scattering

Equation (3) relates a number of physical quantities to the quantity of interest, the distance between viewer and object d . We can obtain information about depth by exploring these relationships.

Take an object immersed in non-vacuous atmosphere. Suppose we take a picture of this object through a color filter, and segment the intensities so that we can obtain average intensities for regions of approximately identical intensities. For each region, this gives us \tilde{C} in equation (3). In order to obtain d , we also need C , the intensity of the object without atmospheric attenuation; β , the extinction coefficient, and S , the sky intensity. We must find ways to handle the four unknowns d , C , β and S in this equation, by measuring some of them separately or by increasing the number of measurements.

We will assume that a single object yields a single equation (3), but in practice we can have several patches of homogeneous intensity in a single object. If

²Such particles produce an extinction coefficient that is larger for red and smaller for blue. This causes the sky to be blue and distant mountains to appear bluish.

two patches are virtually identical, then the two derived equations will be virtually identical and we gain nothing: in this case we should combine the patches and obtain a more reliable intensity average.

The sky intensity S can be measured from any image that contains a portion of the sky. In outdoor images, S is determined by averaging areas of the sky that are far from the Sun. In a laboratory experiment it is possible to obtain S if the atmosphere is densely filled with water vapor, so that distant objects cannot be seen at all (the “sky” intensity is the intensity of an area in which objects are indistinguishable).

If we can measure the illumination of an object with and without scattering effects, we have \tilde{C} and C respectively. We still would need the extinction coefficient β in order to obtain d . Expression (3) yields:

$$\exp(-\beta d) = \frac{\tilde{C} - S}{C - S}. \quad (4)$$

Values of β that are reasonably valid for clean air and different types of fog have been collected [7]. It is unlikely that, in any given experiment, these values will be accurate. Scattering varies significantly with the density and type of particles in the atmosphere, making the precise measurement of β a complex undertaking. Even without β , equation (4) reveals that depth can be extracted up to a multiplicative constant.

If we have several objects, measurement of \tilde{C}_i , C_i and S allows us to obtain relative distances among objects. For each pair of objects:

$$\frac{d_i}{d_j} = \frac{\ln\left(\frac{C_i - S}{\tilde{C}_i - S}\right)}{\ln\left(\frac{C_j - S}{\tilde{C}_j - S}\right)} \quad (5)$$

If we know the depth d_o for an object of known intensity C_o , we can use the object as a “fixed” point. Using expression (5):

$$d_i = K_o \ln\left(\frac{C_i - S}{\tilde{C}_i - S}\right), \quad K_o = \frac{d_o}{\ln\left(\frac{C_o - S}{\tilde{C}_o - S}\right)}.$$

So far we have assumed the possibility of measuring the intensities of objects in the absence of scattering. This is a reasonable assumption when we can make close measurements in clean air. For example, a robot operating in a plant filled with dust, but aware of the form and color of the objects that exist in the plant, or an autonomous vehicle driving in a foggy road, trying to obtain depth cues for the road signs.

For general outdoor environments, objects are distant and produce small disparity; focusing alone cannot distinguish objects that are farther than a certain

m_i	d_i (m)	m_i	d_i (m)
m_1	827	m_2	1635
m_3	2151	m_4	876
m_5	1653		

Table 1: Distance values

distance. On the contrary, light scattering is a depth cue that *benefits* from distance: the farther the object, the larger the effect of scattering.

The problem with outdoor environments is that we cannot measure their intensity *without* the atmosphere. In order to proceed, we will assume that uniform light reaches all areas of the scene and that vegetation and soil characteristics are homogeneous. Under this assumption, we expect all features to have approximately the same intensity were they imaged without scattering.

In this case we can still find useful three-place relations between objects. Consider three objects at distances d_i , d_j and d_k and measured intensities \tilde{C}_i , \tilde{C}_k and \tilde{C}_j respectively. We solve for the ratio of distance differences:

$$\frac{d_i - d_k}{d_j - d_k} = \frac{\ln\left(\frac{\tilde{C}_k - S}{\tilde{C}_i - S}\right)}{\ln\left(\frac{\tilde{C}_k - S}{\tilde{C}_j - S}\right)}. \quad (6)$$

We refer to $\frac{d_i - d_k}{d_j - d_k}$ as the d_k based ratio of d_i to d_j . Expression (6) can be adapted to four objects through similar algebraic manipulations.

4 Outdoor Experiments

We tested expression (6) by taking a series of outdoor images in the area of Pittsburgh, Pennsylvania. Images were taken from a tripod containing a color camera over a rotary platform, a compass, a dual-axis inclinometer and a GPS system [2]. A panorama is formed by merging the images by the Kuglin/Hines method [5, 9]. The top of Figure 2 shows a mosaic made from a sequence of images taken by the river Allegheny. The mountains in the scene are numbered from 1 to 5; we refer to them as m_i , $i \in \{1 \dots 5\}$. Topographic maps were obtained from the United States Geographic Survey (USGS).

The images in Figure 2 were obtained at latitude 40.474350E, longitude 79.965698N. Call d_i the distance from this point to the peak of the mountain m_i ; the ground truth values are given in Table 1.

For each mountain in the panorama, we are interested in the average intensity across the image of the

mountain. We then use these averages as the \tilde{C} values for the mountains in equation (6). The horizon is detected automatically through a search for high gradient pixels; these pixels are assumed to be horizon pixels. The bottom of Figure 2 shows the result of horizon detection. The local maxima of the horizon are then searched, and sequences of pixels are automatically grouped into mountain structures. The average intensity between the horizon and the bottom of the mountains is then calculated (in Figure 2, the average goes from the black horizon line down to the white horizontal line). The average intensities are used in the calculations discussed below.

We studied the accuracy of r_{ij}^k , the d_k ratio of d_i to d_j . The calculation of r_{ij}^k ratios depends on the choice of a mountain m_k which appears in the numerator and denominator; call it the *pivot*. The choice of the pivot is crucial: if the pivot and another mountain are at the same distance from the viewer, the ratio will be grossly miscalculated. For example, we cannot calculate the d_1 ratio of d_2 to d_4 , because d_1 and d_4 are identical for practical purposes. We say two detected mountains “conflict” when their average intensities are approximately the same. A simple algorithm for the choice of a pivot, which uses the information about the horizon obtained above, is:

- average the sky intensity and sort detected mountains by how much their average intensity differs from the sky intensity;
- pick the largest mountain that does not conflict with any other mountain if no mountain can be found under this condition, then pick the largest mountain and discard the conflicting mountains.

In the experiment of Figure 2, there are at most 6 combinations of mountains that can generate ratios for each pivot. We must discard ratios that contain close to zero denominators (caused by conflicts between detected mountains) to avoid numeric instabilities, so the number of mountain combinations may be smaller than 6 in some cases. The following tables show the resulting ratios for three possible pivots, m_3 , m_1 and m_4 respectively. Notice that m_3 is the best pivot since no other mountain conflicts with it. Results are given in Table 2.

The average error in the first table is 9.1%; in the second table, 9.0%, in the third table, 10.5%. Overall, the average error is 9.4%.

We have observed that the effects of scattering vary greatly with atmospheric conditions and the position of the Sun. When sunlight is directly incident on the imaged mountains, scattering effects tend to be buried

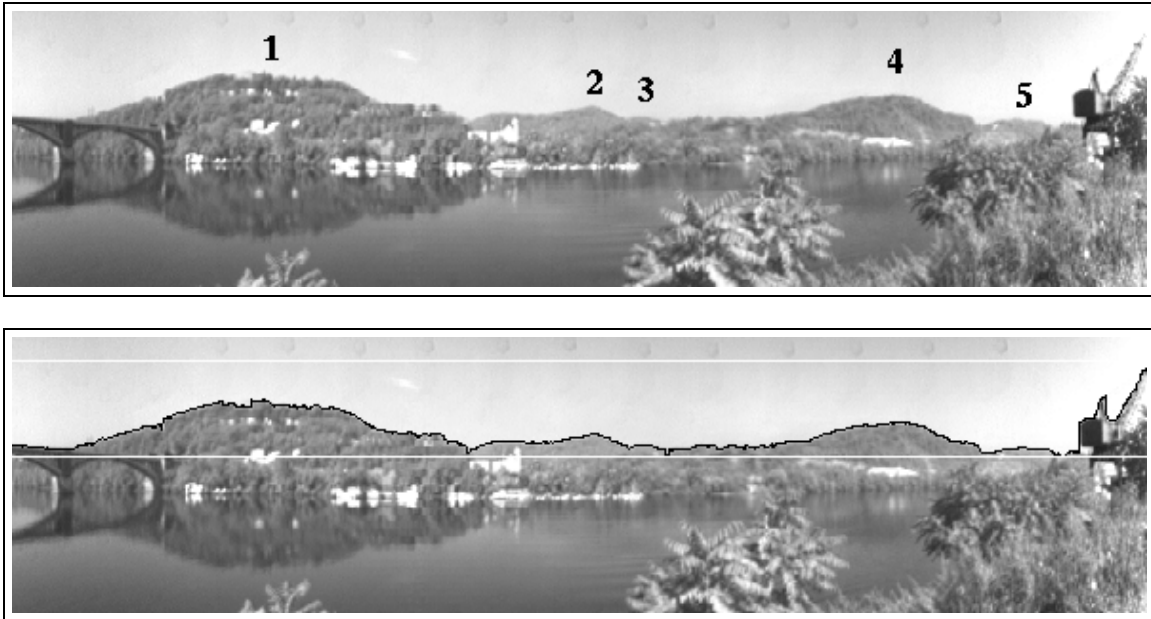


Figure 2: Mosaic with images taken near the Allegheny river

by the extreme brightness of the Sun. Scattering ratios are most effective when the Sun is behind the imaged mountains. The perception and understanding of scattering requires some prior notion of the atmospheric properties of the scenes being imaged; scattering is an additional, powerful depth cue available at little cost for the viewer.

5 Indoor Experiments

Given the promising results of outdoor experiments, the question arises: how well are the assumptions approximated in a small, closed indoor environment?

We studied a small environment to investigate the extent to which our assumptions were valid; we briefly describe our experiment, suggesting some aspects of our work that must receive further testing. We build a rectangular box of size $1.20 \times 0.60 \times 0.25$ meter, with an entry for water vapor and two internal fans for distribution of vapor. Small rectangular, brightly colored objects, were placed in the box and imaged. Figure 3 graphs distance versus average intensity for measurements taken without vapor. The intensity gradually increases as the block receives light from a larger portion of the lamps, reaches a small area of uniform illumination and then decreases. The behavior of such illumination pattern is quite complex, as small changes in the position of the lights caused drastic changes in the intensity values. Such deviations caused errors

Ratio pivot m_3	Ground Truth	Measured	Error
r_{12}^3	0.3900	0.3350	14.1 %
r_{14}^3	0.9628	1.0800	12.2 %
r_{15}^3	0.3762	0.4044	7.5 %
r_{24}^3	0.4051	0.3101	2.3 %
r_{25}^3	0.9647	0.8285	14.1 %
r_{45}^3	0.3908	0.3743	4.2 %

Ratio pivot m_1	Ground Truth	Measured	Error
r_{23}^1	0.6099	0.6649	9.0 %
r_{25}^1	0.9779	1.1100	13.5 %
r_{35}^1	0.6237	0.5955	4.5 %

Ratio pivot m_4	Ground Truth	Measured	Error
r_{23}^4	0.5948	0.6898	15.9 %
r_{25}^4	0.9765	1.1020	12.9 %
r_{35}^4	0.6091	0.6256	2.7 %

Table 2: Results for m_3 , m_1 and m_4 pivots (respectively).

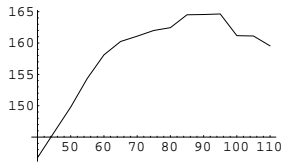


Figure 3: Variations in top illumination with distance

up to ± 20 cm, sometimes even resulting in the wrong order for the blocks. These results indicate that assumption 2 (uniformity of top illumination) cannot be properly enforced in such a small environment.

6 Conclusion

The paper contains an analysis of the physical properties of atmospheric scattering from an image understanding perspective. We presented a physical model for scattering and derived a set of techniques for recovery of depth cues based on scattering measurements. The 10 percent accuracy obtained in outdoor experiments is promising; given the scarcity of depth cues in outdoor environments, such values indicate the possibility of using scattering when performing localization and outdoor image understanding. This is particularly relevant for space applications, in environments with atmosphere but without GPS or similar infrastructure. Experiments with indoor environments of larger dimensions are necessary to study the limits of our assumptions.

Physics based study of atmospheric interactions is an open area for research on the visual perception and understanding of our world; so far the computer vision community has concentrated most of the physical modeling to indoor, clean laboratory settings. Our work opens a number of possible questions for future exploration. For example, one could ask which depth cues can be extracted when single point sources of light are present in the environment. Understanding of outdoor scenery presents great challenges for autonomous, fully situated robots, which must grasp the variations of natural environments in order to interact with them.

A Power and Intensity

Here we sketch the relation between light power and intensity, as they are affected by scattering attenuation. To simplify notation we drop the dependence on wavelength.

Consider an object at distance d from a lens and an image formed at distance $-f$ from the lens. Suppose the lens has diameter l . If we pick a patch δO (with area $A(\delta O)$) in the object, this patch is imaged into a

patch δM (with area $A(\delta M)$) in the image. Consider the line from the center of δM to δO ; call α the angle between this line and the optical axis of the lens and θ the angle between the line and the normal at δO (a similar construction is used by Horn to derive radiometric properties of lenses [3]).

First, since the solid angles of δO and δM must be equal as seen from the lens, we have the equality $\frac{A(\delta O)}{A(\delta M)} = \frac{\cos \alpha}{\cos \theta} \frac{d^2}{f^2}$. Second, the solid angle of the lens as seen from δM is $\frac{\pi l^2 \cos \alpha}{4(d/\cos \alpha)^2}$, and the power through the lens is: $\delta P = LA(\delta O) \cos \theta \exp(-\beta d) \frac{\pi l^2 \cos \alpha}{4(d/\cos \alpha)^2}$, where L is the radiance of the surface.

We are interested in the irradiance, which is measured by the camera sensor and produces the intensity values. Since the irradiance I is $\delta P/A(\delta M)$, we obtain:

$$I = \left(L \frac{\pi l^2}{4 f^2} \cos^4 \alpha \right) \exp(-\beta d) = I_o \exp(-\beta d).$$

References

- [1] E. L. Brown and K. Deffenbacher. *Perception and the Senses*. Oxford University Press, 1979.
- [2] F. G. Cozman and E. Krotkov. Position estimation from outdoor visual landmarks for teleoperation of lunar rovers. *Proc. Third IEEE Workshop on Applications of Computer Vision*, pages 156–161, December 1996.
- [3] B. K. P. Horn. Understanding image intensities. *Artificial Intelligence*, 8(2):201–231, 1977.
- [4] R. V. Klassen. Modeling the effect of the atmosphere on light. *ACM Transactions on Graphics*, 6(3):215–237, July 1987.
- [5] C. D. Kuglin and D. C. Hines. The phase correlation image alignment method. *Proc. of the IEEE Int. Conf. on Cybernetics and Society*, pages 163–165, September 1975.
- [6] N. L. Max. Atmospheric illumination and shadows. *SIGGRAPH*, 20(4):117–123, August 1986.
- [7] E. J. McCartney. *Optics of the Atmosphere*. John Wiley and Sons, Inc., New York, 1976.
- [8] W. E. K. Middleton. *Vision Through the Atmosphere*. University of Toronto Press, 1952.
- [9] R. Szeliski. Image mosaicing for tele-reality applications. Technical Report CRL94/2, DEC Cambridge Research Lab, May 1994.